Bulk Polymerization of Acrylonitrile. II. Model Development

L. H. GARCIA-RUBIO, A. E. HAMIELEC, and J. F. MACGREGOR,
Department of Chemical Engineering, McMaster University, Hamilton, Ontario, Canada

Synopsis

A model for bulk polymerization of AN is developed. It adequately predicts conversion–time histories and molecular weight development in the temperature range of 40°–80°C with AIBN as initiator. It is shown that this model has predictive powers by simulating nonisothermal conversion–time histories.

INTRODUCTION

Heterogeneous bulk polymerizations are processes in which the polymer precipitates from its monomer, giving two loci for polymerization over a large portion of the conversion range, with one being a monomer-rich phase and the other a polymer-rich phase. The physical properties of the polymer and monomer phase have a profound effect on the polymerization rate. In general, heterophase polymerizations are autocatalytic, with an initial acceleration period followed by an almost constant rate period. The rate then increases rapidly, reaching a maximum and then rapidly falling to zero (Fig. 1). The position of the maximum rate is a function of the polymerization conditions and characteristics of the polymer phase.[5,14] The bulk polymerization of acrylonitrile is typical of heterophase processes as shown in part I of this work.[5]

For the description of bulk heterogeneous polymerization, basically two approaches have been suggested. These could be classified as microscopic and macroscopic approaches. The former yields distributed parameter models in which the particles are treated individually as in emulsion polymerization. In this approach some of the important variables, in addition to reaction rate, include number of particles, number of radicals per particle, the rate of absorption and desorption of radicals from the polymer particles, etc. This approach has been suggested by Ugelstadt,[15] Olaj,[9] and Ray[11] for vinyl chloride. This approach is limited to low conversion, where the polymer particles have not experienced appreciable agglomeration. The macroscopic approach does not concern itself with individual particles but rather with the polymerization taking place in the polymer and in the monomer phase as a whole. Its aim is to describe the conversion histories and molecular weight development. This approach was first suggested by Talamini[12] for vinyl chloride and successfully applied to the same polymerization system by Abdel-Alim and Hamielec.[1] Variations of the same have been also successfully applied by Marquardt for acrylonitrile at low conversions.[9] Three polymerization loci have been suggested for acrylonitrile and vinyl chloride: the monomer phase, the polymer phase, and the polymer

Journal of Applied Polymer Science, Vol. 23, 1413–1429 (1979)

0021-8995/79/0023-1413$01.00

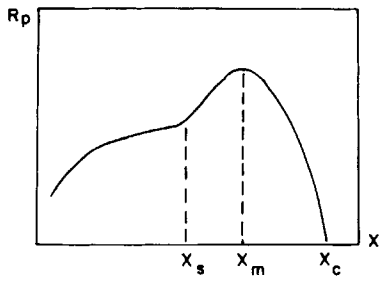

Fig. 1. Typical rate curve for heterogeneous bulk polymerization process.

monomer interface. But in general there is no theory yet available which adequately accounts for the differences observed in vinyl chloride and acrylonitrile bulk polymerization.[5,13]

MODEL DEVELOPMENT

Polymerization Rate Model

The proposed model is based on the following assumptions: (a) there is a monodispersed particle size distribution with a constant number of particles; (b) polymerization takes place in the polymer and monomer phases; and (c) the reactions in the polymer phase are controlled by diffusion of monomer from the onset of the reaction.

These assumptions are supported by experimental evidence. The number of particles has been reported to be fairly constant after approximately 10% conversion.[6,14] The reaction rate has been reported to be independent of the surface area and therefore of the number of particles, which indicates that polymerization occurs in both phases.[6,16] Addition of a swelling agent to the reaction mixture reduces the reaction rate by different amounts for different polymerization conditions. This suggests that the reactions in the polymer phase are diffusion controlled.[14]

A model based on the previous assumptions is a compromise between the macroscopic and microscopic approaches, for although it looks at the individual particles for the description of the polymerization rate, it cannot describe the mechanism by which the particles are formed and it does not account for the change in the number of particles due to agglomeration or continuous generation.

For a monodispersed system with a constant number of particles, an initial mass of monomer with volume V_0 and initial radius R_0 can be associated with each particle. If the particles are heterogeneous, it can be assumed that at time $t > 0$ the polymer particles will have the structure shown in Figure 2, where $4/3\pi(R_0^3 - r_m^3)$ gives the volume shrinkage due to density changes; $4/3\pi(r_m^3 - r_s^3)$ gives the monomer layer at any time t and constitutes the monomer phase; and $4/3\pi(r_s^3 - r_c^3)$ gives the shell or active volume of the polymer phase. At the monomer boundary the composition of the shell is X_s, which corresponds to a monomer-saturated polymer solution at the polymerization conditions. At the core boundary the composition is X_c (limiting conversion), which corresponds to the glass transition composition at the reaction temperature. The polymer

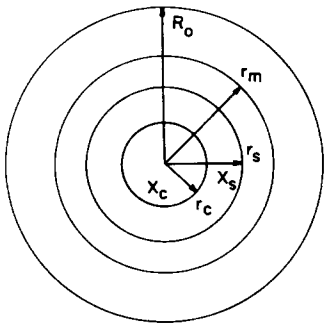

Fig. 2. Structure of a heterogeneous polymer particle.

$4/3\pi r_c^3$ is in the glassy state and, therefore, the polymerization rate within the core is effectively zero.

Rigorously speaking, a concentration gradient should be considered in the shell; but to simplify the analysis, it is assumed to be homogeneous (see discussion in the Appendix).

The following reactions are considered to occur in both phases:

Initiation

$$\begin{aligned} C &\xrightarrow{k_d} 2R_c^{\cdot} \\ R_c^{\cdot} + M &\rightarrow R_1^{\cdot} \end{aligned} \qquad \text{(a)}$$

Propagation

$$\begin{aligned} R_1^{\cdot} + M &\xrightarrow{k_p} R_2^{\cdot} \\ R_n^{\cdot} + M &\xrightarrow{k_p} R_{n+1}^{\cdot} \end{aligned} \qquad \text{(b)}$$

Transfer to monomer

$$R_n^{\cdot} + M \xrightarrow{k_{fm}} P_n + R_1^{\cdot} \qquad \text{(c)}$$

Termination by combination

$$R_n^{\cdot} + R_m^{\cdot} \rightarrow P_{n+m} \qquad \text{(d)}$$

That is, homogeneous kinetics are assumed in each phase. The overall polymerization rate R_{po} is given by the sum of the polymerization rates in the monomer phase R_{pm} and in the shell R_{ps}.

$$R_{po} = R_{pm} + R_{ps} \qquad \text{in moles/sec} \qquad (1)$$

where

$$R_{pm} = k_{pm}\,[R\cdot]_m[M]_m V_m \qquad \text{in moles/sec} \qquad (2)$$

and

$$R_{ps} = k_{ps}\,[R\cdot]_s[M]_s V_s \qquad \text{in moles/sec} \qquad (3)$$

From homogeneous kinetics, if the S.S.H. is assumed valid, a ratio of radical concentrations ξ can be defined as

$$\xi = \frac{[\mathrm{R}\cdot]_s}{[\mathrm{R}\cdot]_m} \tag{4}$$

where

$$\frac{[\mathrm{R}\cdot]_s}{[\mathrm{R}\cdot]_m} = \frac{(2f_s k_{ds}[I]_s)^{1/2}/k_{ts}{}^{1/2}}{(2f_m k_{dm}[\mathrm{I}]_m)^{1/2}/k_{tm}{}^{1/2}} \tag{5}$$

where the subscripts s and m denote the shell and monomer phases, respectively, and f is the efficiency of the initiator. A mass balance of the initiator in the polymer and monomer phases, assuming that the core and shell have the same initiator concentration, gives

$$[\mathrm{I}] = [\mathrm{I}]_m \frac{V_m}{V_T} + [\mathrm{I}]_s \left(\frac{V_s + V_c}{V_T}\right) \tag{6}$$

Introducing the initiator partition coefficient

$$K_\mathrm{I} = \frac{[\mathrm{I}]_s}{[\mathrm{I}]_m} \tag{7}$$

combining eqs. (6) and (7), and substituting the concentrations into eq. (5) yields

$$\xi = \left(\frac{f_s}{f_m} K_\mathrm{I} \frac{k_{ds}}{k_{dm}} \frac{k_{tm}}{k_{ts}}\right)^{1/2} \tag{8}$$

To use eqs. (1)–(8), a value of the initiator partition coefficient must be assumed. A reasonable assumption appears to be $K_\mathrm{I} = 1$, since this value can be inferred from an experiment reported in reference (2) and it has given good results for VC Bulk polymerization over a wide range of conditions (1). Under this assumption combining equation (1) to (8) yields:

$$R_{po} = \left(\frac{R_{\mathrm{I}m}}{k_{tm}}\right)^{1/2} (k_{pm}\,[\mathrm{M}]_m V_m + k_{ps}[\mathrm{M}]_s V_s \xi) \tag{9}$$

where

$$R_{\mathrm{I}m} = 2f_m\, k_{dm} \frac{[\mathrm{I}]_0}{(1 - QX)} \exp\,(-k_d t) \tag{10}$$

$$Q = \frac{\rho_p - \rho_m}{\rho_p} \tag{11}$$

Q is the correction due to volume contraction.

Since the shell has been considered homogeneous throughout the reaction, a constant ratio of propagation rate constants can be assumed:

$$\lambda = \frac{k_{ps}}{k_{pm}} \tag{12}$$

Then the polymerization rate is given by

$$R_{po} = \left(\frac{k_{pm}}{k_{tm}{}^{1/2}}\right) \left[2f_m k_d \frac{[\mathrm{I}]_0}{(1 - QX)} \exp\,(-k_d t)\right]^{1/2} ([\mathrm{M}]_m V_m + [\mathrm{M}]_s V_s \lambda \xi) \tag{13}$$

In order to solve eq. (13), it is necessary to derive expressions for the terms

$[M]_m V_m$ and $[M]_s V_s$. A material balance on the polymer particle under the assumption of homogeneous core and shell gives the monomer concentrations and the volumes of the monomer phase and the shell. The density of the shell is given by

$$\frac{1}{\rho_s} = \frac{1}{\rho_m}(1 - X_s Q) \tag{14}$$

and the density of the core by

$$\frac{1}{\rho_c} = \frac{1}{\rho_m}(1 - X_c Q) \tag{15}$$

The initial volume per particle is given by

$$V_0 = \frac{4}{3}\pi R_0^3 = \frac{M_0}{\rho/\overline{M}} \qquad \text{in liters/particle} \tag{16}$$

where M_0 is in gmol of monomer/particle, ρ is the density of monomer in 2/l, and $\overline{M}$ is the monomer molecular weight in g/gmol.
At any conversion X, the volume of the particle is given by

$$V = V_0(1 - QX) \quad \text{or} \quad r_m^3 = \frac{3}{4}\frac{V_0}{\pi}(1 - QX) \quad \text{in liters/particle} \tag{17}$$

An overall mass balance on the particle gives

$$(\rho_c - \rho_s)r_c^3 + (\rho_s - \rho_m)r_s^3 + \rho_m r_m^3 = \rho m R_0^3 \tag{18}$$

Solving for r_s^3 yields

$$r_s^3 = \left(\frac{\rho_m}{\rho_s - \rho_m}\right) R_0^3 Q X - \left(\frac{\rho_c - \rho_s}{\rho_s - \rho_m}\right) r_c^3 \tag{19}$$

The total mass balance of monomer in the monomer phase is given by

$$[M]_m V_m = \frac{4}{3}\pi \frac{\rho_m}{\overline{M}}(r_m^3 - r_s^3) \tag{20}$$

Combining eqs. (18) and (20)

$$[M]_m V_m = \frac{4}{3}\pi \frac{\rho_m}{\overline{M}}\left(R_0^3 - \frac{\rho_s}{\rho_m} r_s^3 - \frac{\rho_c - \rho_s}{\rho_m} r_c^3\right) \tag{21}$$

Similarly, the total mass of monomer in the shell might be given by

$$[M]_s V_s = \frac{4}{3}\pi \frac{\rho_s}{\overline{M}}(r_s^3 - r_c^3)(1 - X_s) \tag{22a}$$

However, this equation is rigorous only if the shell has a constant monomer concentration. To account for the concentration gradients, the mass balance on the shell, eq. (A-1), must be solved in conjunction with eqs. (13), (19), and (21). As discussed in the Appendix, this approach leads to the following approximation to the mass of monomer in the shell:

$$[M]_s V_s = \frac{4}{3}\pi R_0^3 \frac{\rho_s}{\overline{M}}(1 - X_s)\phi B(X) \tag{22b}$$

where $B(X)$ is a beta function (given in the Appendix) used to describe the rel-

ative rate of growth of the core and shell volumes, and ϕ is an unknown function of the initiation rate.

Substituting eqs. (21) and (22b) into eq. (13) and taking the definition of rate in terms of conversion, a final expression for the polymerization rate is obtained:

$$\frac{dX}{dt} = C_p R_{Im}{}^{1/2}\left[1 - \frac{\rho_c Q X}{\rho_c - \rho_m} - B(X)\left(\left(\frac{\rho_c - \rho_s}{\rho_c - \rho_m}\right) - P\frac{(1-X)}{\rho_m}\rho_s\right)\right] \quad (23)$$

where

$$C_p = \frac{k_{pm} f_m{}^{1/2}}{k_{tm}{}^{1/2}} \qquad \text{and} \qquad P = \xi\lambda\phi$$

Since at X_M

$$\frac{d^2X}{dt^2} = 0 \quad (24)$$

the value of P can be calculated by taking the derivative of eq. (23) and equating it to zero:

$$P = \frac{\gamma + \left(\dfrac{\rho_c}{\rho_c - \rho_m}\right)(2 - QX_M) - 1}{C_s \dfrac{\overline{\mathrm{M}}}{\rho_m} B(X_\mathrm{M})} + \frac{(\rho_c - \rho_s)\rho_m}{(\rho_c - \rho_m) C_s \overline{\mathrm{M}}} \quad (25)$$

where

$$C_s = (1 - X_s)\frac{\rho_s}{\rho_m} \quad (26)$$

and

$$\gamma = \frac{k_d}{Q}\frac{(1 - QX_\mathrm{M})}{C_P R_{\mathrm{It}\mathrm{M}}{}^{1/2}} \quad (27)$$

It can be seen from eq. (25) that P is a function of the initiation rate and characteristics of the polymer phase at the reaction conditions (Fig. 3). $R_{It\mathrm{M}}$ and $B(X_\mathrm{M})$ are given by eqs. (10) and (A-2) evaluated at X_M.

Equation (23) is a nonlinear differential equation that can be integrated by any standard technique. The parameters in this equation are k_d, C_p, and X_M. These parameters were estimated by nonlinear regression using the experimental conversion–time results reported in part I of this work; k_d and C_p were estimated in an Arrhenius form. The activation energies and frequency factors are reported in Table I. The values obtained for k_d are in agreement with the well-known values reported elsewhere.[1] The values of X_M were estimated initially for each temperature and initiator concentration in order to find an empirical correlating relationship for it with the process variables, namely, initiation rate (Fig. 4) and temperature (Fig. 5). Finally, all the parameters (k_d, C_p, and the parameters of the correlating relationship for X_M) were estimated using all the data at different temperatures and initiator concentrations. The resultant values are reported in Table I.

The model with the parameters thus obtained gives a very good fit of the experimental data. Figures 6–8 show the comparison between experimental and

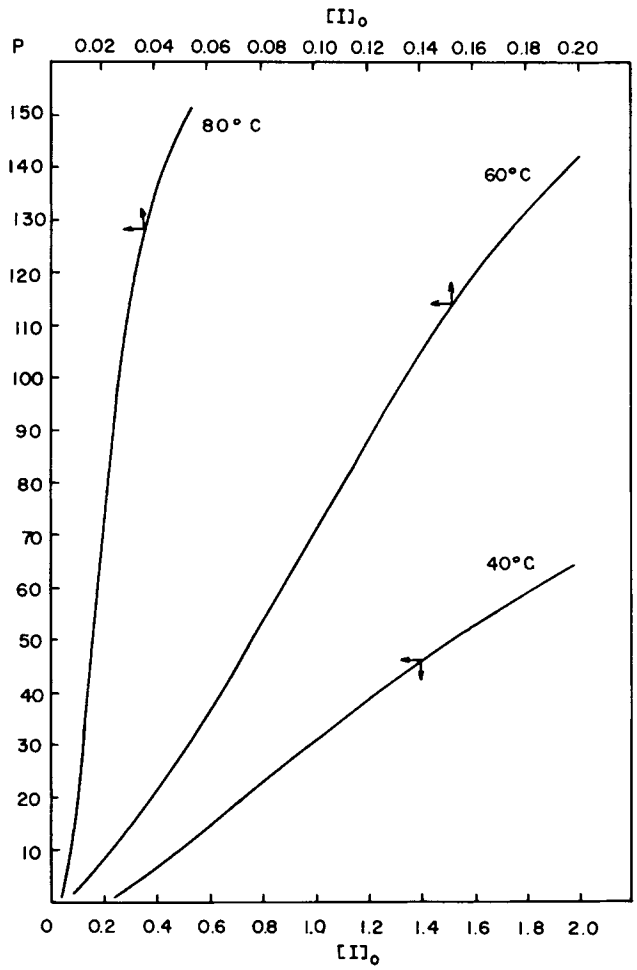

Fig. 3. P values for several initiator concentrations and temperatures.

calculated values at several initiator concentrations and temperatures. The rate behavior for AN reported in part I has been satisfactorily reproduced by the model (Fig. 9). The model was further tested by running nonisothermal polymerizations to determine whether it had any predictive power or was just a form of curve fitting. The reactions were run isothermally for a period of time, and then the ampoules were changed to another bath at a higher temperature. The model predictions and the experimental results are shown in Figure 10; the agreement is quite good.

Molecular Weight Distribution

Due to the heterogeneous nature of the reaction in acrylonitrile bulk polymerization, termination reactions can take place in the monomer phase, the polymer phase, and the polymer–monomer interphase. In the monomer phase, bimolecular termination can be important, as it has been reported for homogeneous polymerizations of acrylonitrile.[3] At the interphase bimolecular termi-

TABLE I
Kinetic Parameters for Acrylonitrile Bulk Polymerization with AIBN Initiator in the Temperature Range of 40°–80°C

(1) Polymerization Rate Model Parameters

$$k_d = 1.65 \times 10^{-6} \exp\left[\frac{-30720}{R}\left(\frac{1}{T} - \frac{1}{333.16}\right)\right] \text{ sec}^{-1}$$

$$C_p = 0.1969 \exp\left[\frac{-3570}{R}\left(\frac{1}{T} - \frac{1}{333.16}\right)\right] \left(\frac{\text{sec moles}}{\text{liter}}\right)^{-1/2}$$

(2) MWD Model Parameters

$$C_m = 7.2063 \times 10^{-5} \exp\left[\frac{-3222}{R}\left(\frac{1}{T} - \frac{1}{333.16}\right)\right]$$

$$A = 9.15 - 0.0962(T - 273.16)$$

(3) Other Correlations

$$X_c = -2.355 + 0.01816T - 0.25 \times 10^{-4}T^2$$

$$X_s = 0.5468 + 0.001T$$

$$X_M = X_{M_0} \exp\left(E_{X_M}/\sqrt{R_{I_0}}\right)$$

$$X_{M_0} = -0.026 + 0.0543(T - 273.16)$$

$$E_{X_M} = (1.109 \times 10^4) - (0.1745 \times 10^{-5})\,(T - 273.16) \qquad T \text{ in °K}$$

nation is also possible for radicals that have not been completely immobilized.[6] In the polymer phase, however, it is very unlikely that bimolecular reactions are important, since the polymer is almost at its glassy state and the radicals are immobilized.[3] Termination can then take place by transfer to monomer[4] or an equivalent mechanism.[14] Since all these mechanisms can be important at different stages during the reaction, it is very difficult to assess which one controls the overall MWD.

In developing the model for the MWD and averages, the following considerations were made:

(1) Because of its high reaction rates, most of the polymer is produced or grows

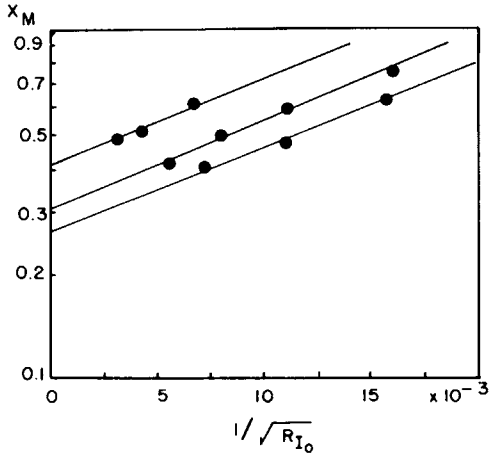

Fig. 4. Conversion at maximum rate vs initial initiation rate.

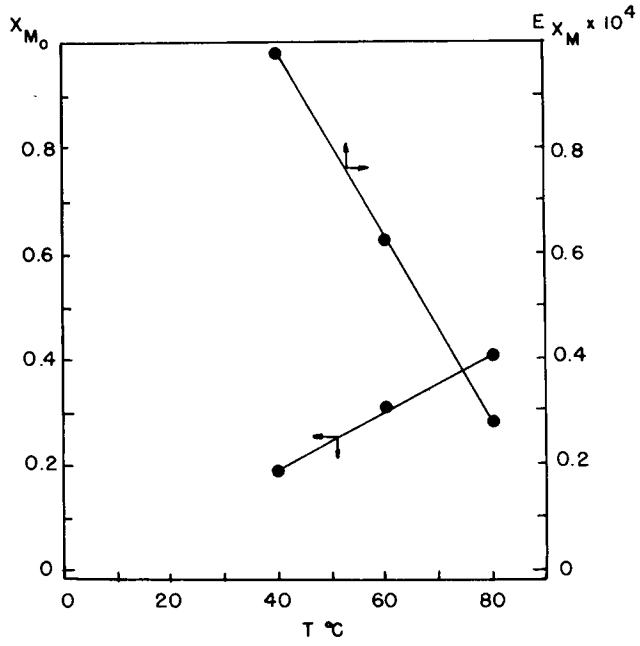

Fig. 5. Dependency of the parameters X_{M_0} and E_{X_M} on temperature for the equation $X_M = X_{M_0} \exp(E_{X_M}/\sqrt{R_{I_0}})$.

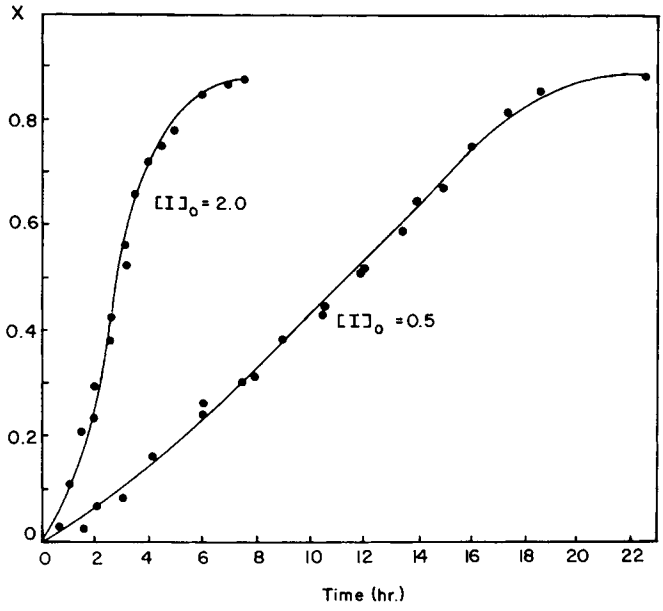

Fig. 6. Acrylonitrile bulk polymerization at 40°C.

in the polymer phase. Therefore, the overall MWD can be approximated by the MWD generated in the polymer phase.

(2) It is assumed that transfer to monomer controls the MWD in the polymer phase. But since reactions in the polymer phase are diffusion controlled, k_{fm}/k_p is a function of conversion.

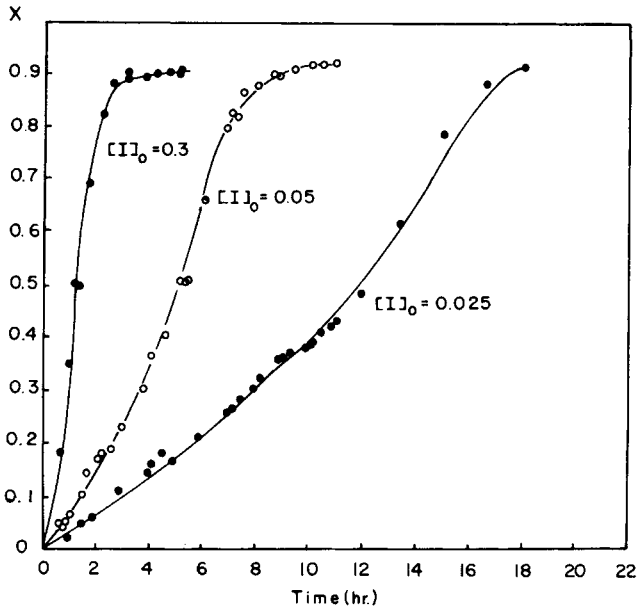

Fig. 7. Acrylonitrile bulk polymerization at 60°C.

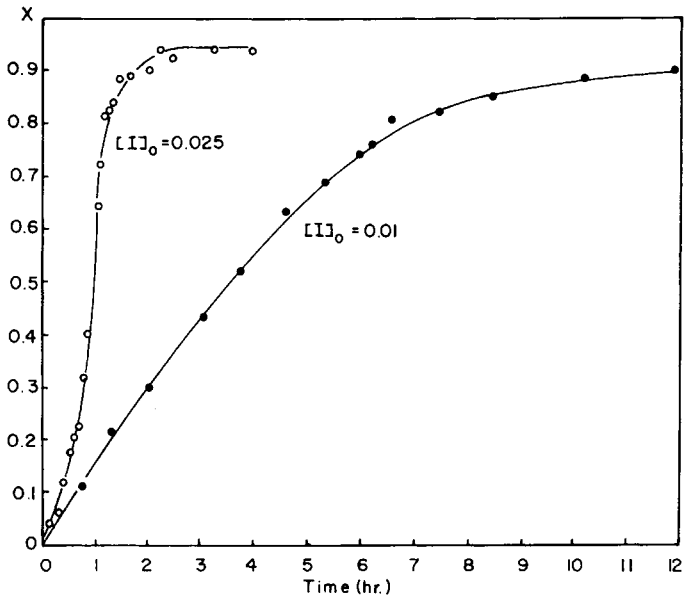

Fig. 8. Acrylonitrile bulk polymerization at 80°C.

From the theory of homogeneous kinetics applied to the polymer phase, the instantaneous weight fraction of polymer with chain length r is given by

$$w(r,t) = (\tau + \beta)\,[\tau + \tfrac{1}{2}\beta(\tau + \beta)r]r \exp\,[-(\tau + \beta)r] \tag{28}$$

where

$$\tau = \frac{k_{fm}}{k_p} + \frac{k_{td}R_p}{k_p^2[\mathrm{M}]^2} \tag{29}$$

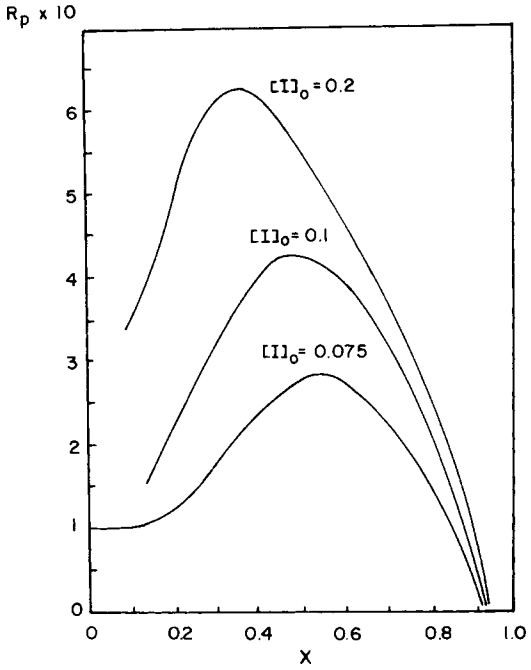

Fig. 9. Polymerization rate at 60°C.

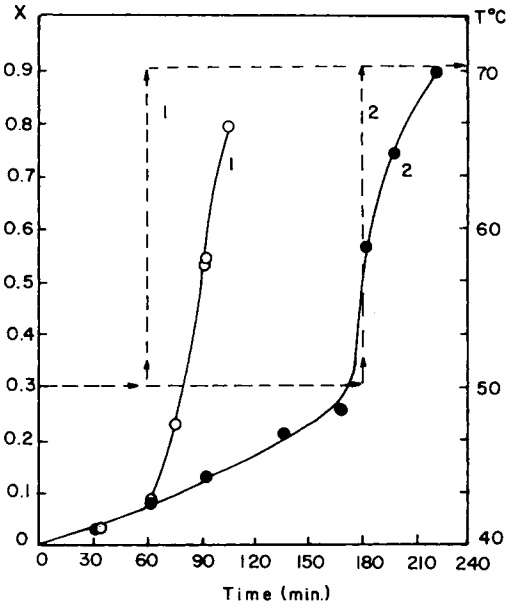

Fig. 10. Nonisothermal bulk polymerization of acrylonitrile at two temperature levels: 50°C and 70°C: $[I]_0$ = 0.2 wt-%; (○),(●) experimental values; (1) run No. 1; (2) run No. 2; (—) model; (- - -) temperature profile.

$$\beta = \frac{k_{tc}R_p}{k_p^2[\mathrm{M}]^2} \tag{30}$$

under the above assumptions

$$\tau = \frac{k_{fm}}{k_p} \tag{31}$$

$$w(r,t) = \tau^2 r\, e^{-\tau r} \tag{32}$$

We assume the conversion dependence of k_{fm}/k_p to be of the form

$$\frac{k_{fm}}{k_p} = \left(\frac{k_{fm}}{k_p}\right)_0 + C_T\,(1 - X)$$

then

$$\tau = C_{m_0} + C_T\,(1 - X) \tag{33}$$

Note that since we are approximating the overall MWD with that produced in the polymer phase, the term $C_T(1 - X)$ includes not only the diffusion effects but also the extent of bimolecular termination in the monomer phase and at the polymer–monomer interphase.

Instantaneous average chain lengths are given by

$$\bar{r}_N = 1/\tau \tag{34}$$

$$\bar{r}_w = 2/\tau \tag{35}$$

and cumulative weight fraction and chain length averages by

$$w_c(r) = \frac{1}{X}\int_0^X w(r,t)\,dX \tag{36}$$

$$\bar{r}_{N_c} = \frac{X}{\displaystyle\int_0^X \frac{1}{\bar{r}_N}\,dX} \tag{37}$$

$$\bar{r}_{w_c} = \frac{1}{X}\int_0^X \bar{r}_w\,dX \tag{38}$$

Substituting eqs. (33)–(35) into eqs. (36)–(38) yields

$$w_c(r) = \frac{C_{m_0}^2}{X}\int_0^X [1 + A\,(1 - X)]^2 r \exp\left(-C_{m_0}[1 + A\,(1 - X)r)\right] dX \tag{39}$$

$$\bar{r}_{w_c} = \frac{2}{XAC_{m_0}} \ln\left(\frac{1}{1 - \dfrac{AX}{1 + A}}\right) \tag{40}$$

$$\bar{r}_{N_c} = \frac{1}{C_{m_0}\left[1 + \dfrac{A}{2}\,(2 - X)\right]} \tag{41}$$

where

$$A = \frac{C_T}{C_{m_0}}$$

The MWD and averages are functions, therefore, of two temperature-dependent parameters (C_{m_0} and A) and conversion. Since the difference in mo-

lecular weights due to initiator concentrations is not significant, the parameters were not correlated with respect to initiator concentration; C_{m_0} and A were estimated from the molecular weight averages reported in part I.[5] The model predictions and experimental results are shown in Figures 11–13. The agreement was satisfactory. The parameters C_{m_0} and A are reported in Table I in their functional form. The parameter C_{m_0} represents the ratio transfer to monomer to propagation without any effect of conversion. It is interesting that the values obtained for C_{m_0} are in agreement with values reported in the literature,[17] thereby indicating that the assumptions made in deriving the MWD model are probably not unreasonable.

A flow diagram describing the use of the model is shown in Figure 14. The computer program is available upon request.

DISCUSSION

On the basis of the proposed model, it is possible to explain some of the differences observed between acrylonitrile and vinyl chloride bulk polymerization processes. In general, the core formation is a function of the initiation rate and the properties of the system at the polymerization conditions (X_c, X_s, ρ_p, etc.), and its rate of growth increases with increasing initiator concentration. Therefore, a high initiation rate will favor the growth of the core and reduce the volume available for polymerization in the polymer phase. The rate will increase

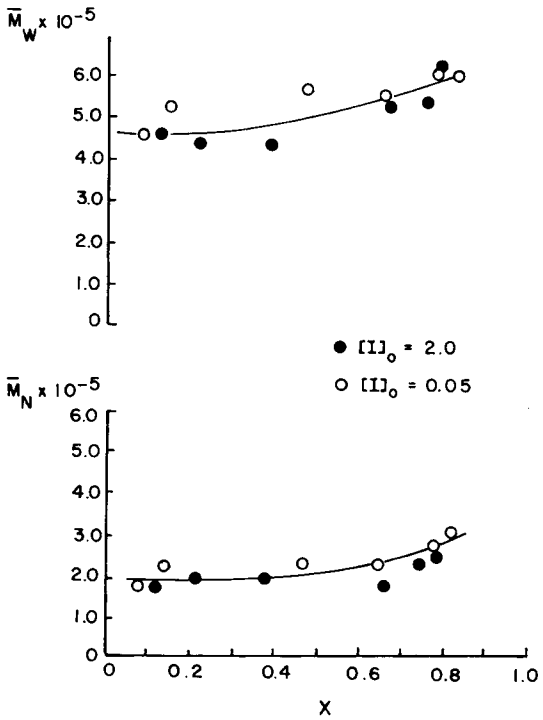

Fig. 11. Molecular weight averages vs conversion at 40°C: (●) $[I]_0 = 2.0$; (○) $[I]_0 = 0.05$.

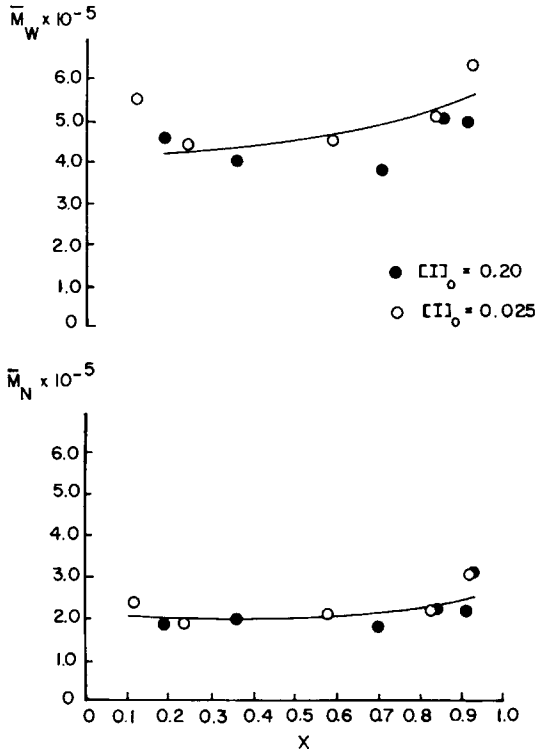

Fig. 12. Molecular weight averages vs conversion at 60°C: (●) $[I]_0 = 0.20$; (○) $[I]_0 = 0.025$.

rapidly at the beginning of the polymerization up to the point where the core is formed and begins to grow, thereby decreasing the reaction rate. In the case of acrylonitrile, as the initiation rate is decreased the growth of the core is retarded and the maximum rate appears later in conversion. For vinyl chloride, the high solubility of the monomer in the polymer precludes monomer diffusion control, and the polymer phase can be considered homogeneous. It has been reported, however, that vinyl chloride follows the same behavior as acrylonitrile when polymerized at low temperatures and high initiation rates.[13] Furthermore, it is evident from Meeks' data at normal temperatures[8] that an early maximum appears with vinyl chloride at high initiation rates. In this case, after a rapid growth of the core the initiation rate decreases due to initiator consumption, the thermodynamic equilibrium is restored, and the reaction then follows this equilibrium path. The same reasoning applies to the number of radicals trapped in the polymer phase. The aftereffect will be more considerable for polymer produced at low temperatures and high initiation rates.

The relative growth of the core and shell accounts also for the discrepancies regarding the reported polymerization loci for acrylonitrile, since at low initiation rates the system behaves like a two-phase system with practically homogeneous polymer particles, as proposed by Marquardt.[7] At high initiation rates the core and shell boundaries will be very close, with the result that the reaction takes place practically at the polymer–monomer interface as suggested by Peebles[10] and Lewis and King.[6]

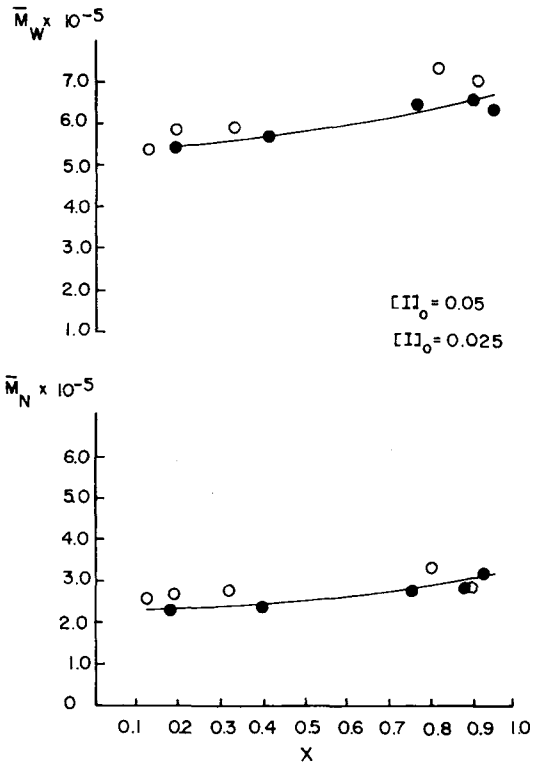

Fig. 13. Molecular weight averages vs conversion at 80°C: (●) $[I]_0 = 0.05$; (●) $[I]_0 = 0.025$.

Appendix

Relative Growth of The Core and Shell

For the rigorous solution of eqs. (13), (19), and (21), it is necessary to include the monomer concentration gradients within the shell given by the continuity equation:

$$\frac{\partial [M]_s}{\partial t} = D\left[\frac{1}{r^2}\frac{\partial}{\partial r}\left(r^2\frac{[M]_s}{\partial r}\right)\right] - k_{p_s}[R\cdot]_s[M]_s \tag{A-1}$$

with boundary conditions

$$r = r_c \qquad [M]_s = (1 - X_c)\rho_c/\bar{M}$$

$$r = r_s \qquad [M]_s = (1 - X_s)\rho_s/\bar{M}$$

$$t = 0 \qquad r = r_s = r_c = 0$$

This system has the following initial and final conditions:

$$\text{at} \quad t = 0 \qquad r_m = R_0$$

$$\text{at} \quad t = \infty \qquad r_m = r_s = r_c$$

Note that eqs. (13), (19), (21), and (A-1) form a coupled moving boundary system which is very difficult to solve. From the constrained solution of this system of equations at each initiator level and the form of the rate curves, it was found that the relative growth of the core and shell could be approximated by a beta function such that

$$\frac{r_s^3 - r_c^3}{R_0^3} = B(X) = DY^{p-1}(1 - Y)^{g-1} \tag{A-2}$$

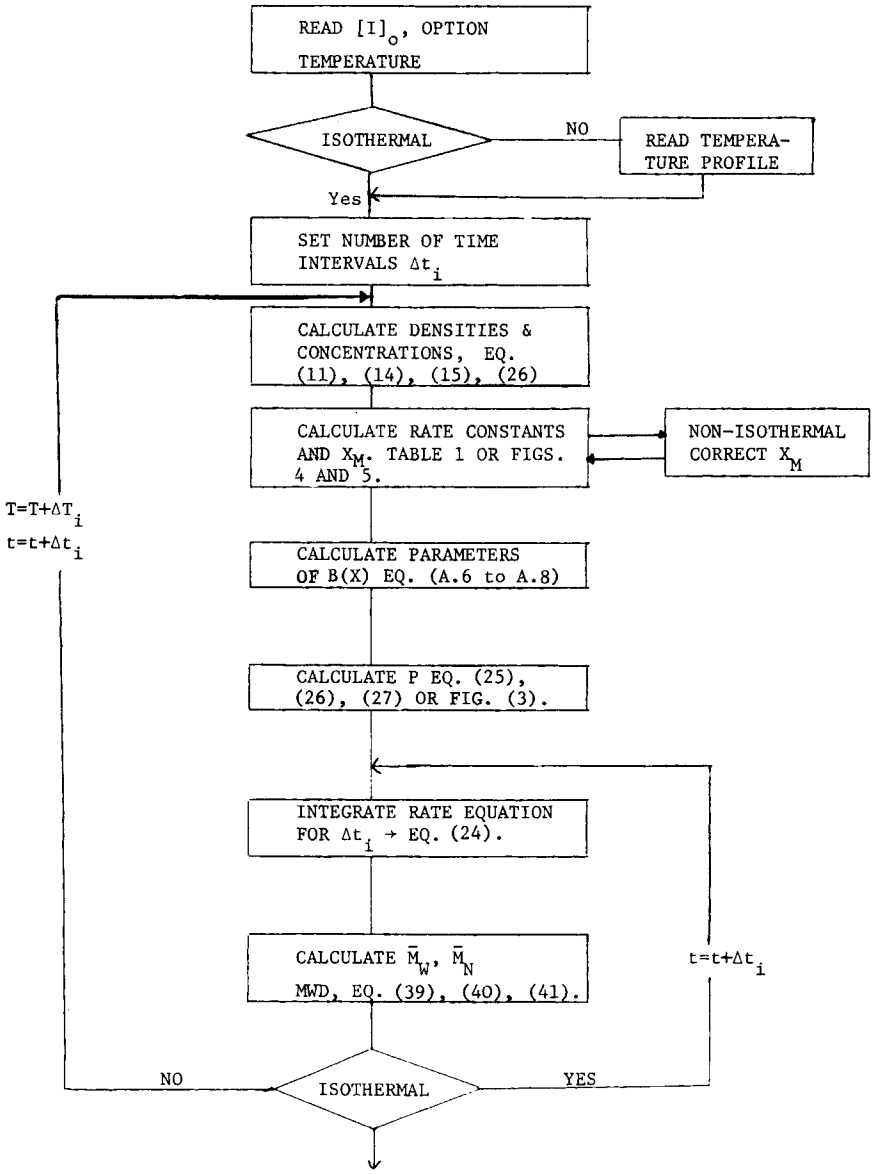

Fig. 14. Model flow diagram for the calculations of isothermal and nonisothermal conversion histories and MWD.

where

$$Y = \frac{X}{X_c}$$

and that the monomer in the shell ($[M]_s V_s$) could also be approximated at any time for each initiator level by assuming a constant monomer concentration (at conversion X_s) and using eq. (A-2) to calculate V_s, that is,

$$[M]_s V_s \Big|_{[I]_0} = \frac{4}{3}\pi \frac{\rho_s}{\bar{M}} (1 - X_s) R_0^3 B(X) \Big|_{[I]_0} \tag{A-3}$$

Furthermore, it was also found that $B(X)_{[I]_0}$ varied with initiator concentration at each temperature level, and therefore eq. (A-3) could be written in general as

$$[M]_s V_s = \frac{4}{3}\pi \frac{\rho_s}{\overline{M}}(1 - X_s)R_0^3 B(X)\phi \tag{A-4}$$

where ϕ is a function of the initiator concentration at each temperature level, and it is to be determined from the rate expression.

The parameters D, p, and g of the beta function in eq. (A-2) can be determined by the following conditions: (1) The position of the mode is given by the conversion at which the rate is maximum (X_M). (2) Equation (A-2) must satisfy eq. (19) at X_0, the conversion at which the core begins to grow. (3) Equation (A-2) must also pass through any arbitrarily chosen point X_i between $X = 0$ and $X = X_0$ for which $r_c = 0$ if the material balance given by eq. (19) is to be satisfied.

From the first condition,

$$\frac{dB(X)}{dY} X_M = 0 \tag{A-5}$$

which gives

$$g - 1 = (p - 1)\left(\frac{X_c - X_M}{X_M}\right) \tag{A-6}$$

Evaluating eqs. (19) and (A-4) at X_0 and X_1 and solving for D and p yields

$$p - 1 = \frac{\ln\left(\frac{X_0}{X_1}\right)}{\ln\left(\frac{X_0}{X_1}\right) + \left(\frac{X_c - X_M}{X_M}\right)\ln\left(\frac{X_c - X_0}{X_c - X_1}\right)} \tag{A-7}$$

and

$$D = \frac{\rho_m}{\rho_s - \rho_m} \frac{Q X_0}{\left(\frac{X_0}{X_c}\right)(p - 1)\left(\frac{X_c - X_0}{X_c}\right)(g - 1)} \tag{A-8}$$

If the drop in the polymerization rate after X_M is assumed to be due to the beginning of core growth, then

$$X_0 = X_M \tag{A-9}$$

and

$$X_1 = \psi X_M \tag{A-10}$$

where ψ is any fraction less than 1 according to condition (3).

References

1. A. Abdel-Alim, and A. E. Hamielec, *J. Appl. Polym. Sci.*, **16,** 783 (1972).
2. C. H. Bamford and A. Jenkins, *Proc. R. Soc., London, Ser. A* **216,** 515 (1953).
3. C. H. Bamford, A. Jenkins, and R. Johnstone, *Trans. Faraday Soc.*, **55,** 1777 (1959).
4. L. H. Garcia-Rubio, M. Eng. Thesis, McMaster University, 1975.
5. L. H. Garcia-Rubio and A. E. Hamielec, *J. Appl. Polym. Sci.*, **23,** 1397 (1979).
6. O. G. Lewis and R. M. King, *Adv. Chem. Ser.*, **91,** (1969).
7. K. Marquardt and P. Mehnert, *Makromol. Chem.*, **28,** 177 (1974).
8. M. R. Meeks, *Polym. Eng. Sci.*, **9,** 141 (1969).
9. O. F. Olaj, *Makromol. Chem.*, **47,** 1 (1975).
10. L. H. Peebles, Jr., *Copolymerization*, Interscience, New York, 1964, Chap. 9.
11. W. H. Ray and S. K. Jain, *J. Appl. Polym. Sci.*, **19,** 1297 (1975).
12. G. Talamini and G. Vidotto, *Makromol. Chem.*, **53,** 21 (1962).
13. M. Tavan, et al., *J. Polym. Sci.*, **12,** 411 (1974).
14. W. M. Thomas, *Adv. Polym. Sci.*, **2,** 401 (1961).
15. J. Ugelstadt, et al., *Makromol. Chem.*, **164,** 171 (1973).
16. S. Yamasaki, M. Fukuda, and M. Namaskima, *Kobunshi Kagaku*, **27,** 459 (1970).
17. J. Brandrup and E. N. Immergut, Eds., *Polymer Handbook*, Interscience, New York, 1975.

Received July 27, 1977
Revised February 24, 1978